International Journal of Minerals, Metallurgy and Materials
Volume 17, Number 6, December 2010, Page 763
DOI: 10.1007/s12613-010-0386-5

FEM analysis of metal flowing behaviors in porthole die extrusion based on the mesh reconstruction technology of the welding process

Dong-nan Huang[1,2], *Zhi-hao Zhang*[1], *Jing-yuan Li*[1], *and Jian-xin Xie*[1]

1) Advanced Materials and Technologies Institute, University of Science and Technology Beijing, Beijing 100083, China
2) School of Materials Science and Engineering, Inner Mongolia University of Technology, Huhhot 010051, China
(Received: 16 May 2010; revised: 13 July 2010; accepted: 15 July 2010)

Abstract: A reconstruction technology of finite element meshes based on reversal engineering was applied to solve mesh penetration and separation in the finite element simulation for the divergent extrusion. The 3D numerical simulation of the divergent extrusion process including the welding stage for complicated hollow sections was conducted. Based on the analysis of flowing behaviors, the flowing velocities of the alloy in portholes and near the welding planes were properly controlled through optimizing the expansion angle as well as porthole areas and positions. After the die structure optimization, defects such as warp, wrist, and the wavelike are eliminated, which improves the section-forming quality. Meanwhile, the temperature distribution in the cross section is uniform. Especially, the temperature of the C-shape notch with a larger thickness is lower than that of other regions in the cross section, which is beneficial for balancing the alloy flowing velocity.

Keywords: numerical simulation; extrusion; metal forming; metal flow; reconstruction

1. Introduction

Only dependent on traditional methods that are based on the personal experiences of the designers, it is difficult to design the structure and dimensions of divergent extrusion die for the products with a complicated hollow cross section [1-2]. The main reason is that the uniformity of metal flowing velocities can not be controlled correctly. However, it is easy to analyze the flowing behaviors of metal during the extrusion process and predict the quality of the section by adopting numerical simulation [3-5]. Optimizing the die structure and dimensions as well as extrusion processes can improve the production efficiency and lower the cost [6-8].

However, the present finite element method (FEM) can only simulate the dividing or steady-forming stage of the divergent extrusion for the complicated cross-section sample and welding plane that is not in the flowing symmetry plane [9-11]. Because the welding stage including the whole process of extrusion is hard to be simulated by the traditional FEM technology, the effects of the porthole configuration, the structure of the welding chamber, and the welding angle on metal flowing behaviors and welding quality can not be analyzed. By using the finite volume method, although the welding stage of divergent extrusion can be simulated [12], it is unable to simulate the twisting and warp of the sections caused by the non-uniform flowing velocity of the metals in two sides of the welding plane because of the separation of the mesh nodes in the welding plane in this method.

Consequently, approaching a method to simulate the whole extrusion process (including the welding stage) of the complicated hollow section is of great significance to design the structure of the die reasonably and effectively. Meanwhile, it is the essential prerequisite to replace the die-testing process, which is necessary in the traditional die design. A reconstruction technology of finite element meshes based on reverse engineering [13] is proposed in this paper and mesh penetration and separation in the divergent extrusion simulation are successively avoided. The application of the reconstruction technology in divergent extrusion for a simple cross section and the experimental test for its reliability were reported in Ref. [14].

Corresponding author: Jian-xin Xie E-mail: jxxie@mater.ustb.edu.cn

In this paper, based on our previous work, the effects of the structure and dimensions of an industrial section with a complicated hollow cross section on the metal flowing behaviors were analyzed. The forming quality of the section was also predicted according to the temperature distributions of the cross section.

2. Numerical simulation

2.1. Die structure and boundary conditions

Fig. 1 indicates the structure and dimensions of an industrial section with two cavities, one U-type notch (left side) and one C-type notch (right side). The area of the cross section is 1435.5 mm^2. The thickness of the C-type notch end is larger than that of other regions.

The model of the porthole die is shown in Fig. 2. The upper die has eight portholes, two mandrels and one drain hole. The outline of the welding chamber of the bottom die is the same as that of the upper die.

It is assumed that A6005 aluminum alloy at high temperature is plastic material and the die is rigid material.

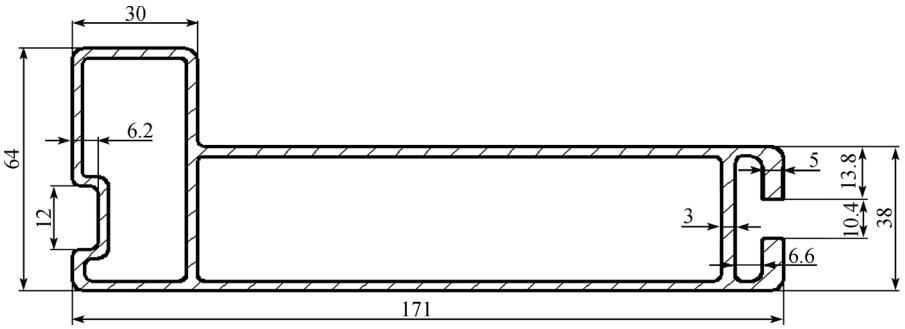

Fig. 1. Structure and dimensions of an industrial section (unit: mm).

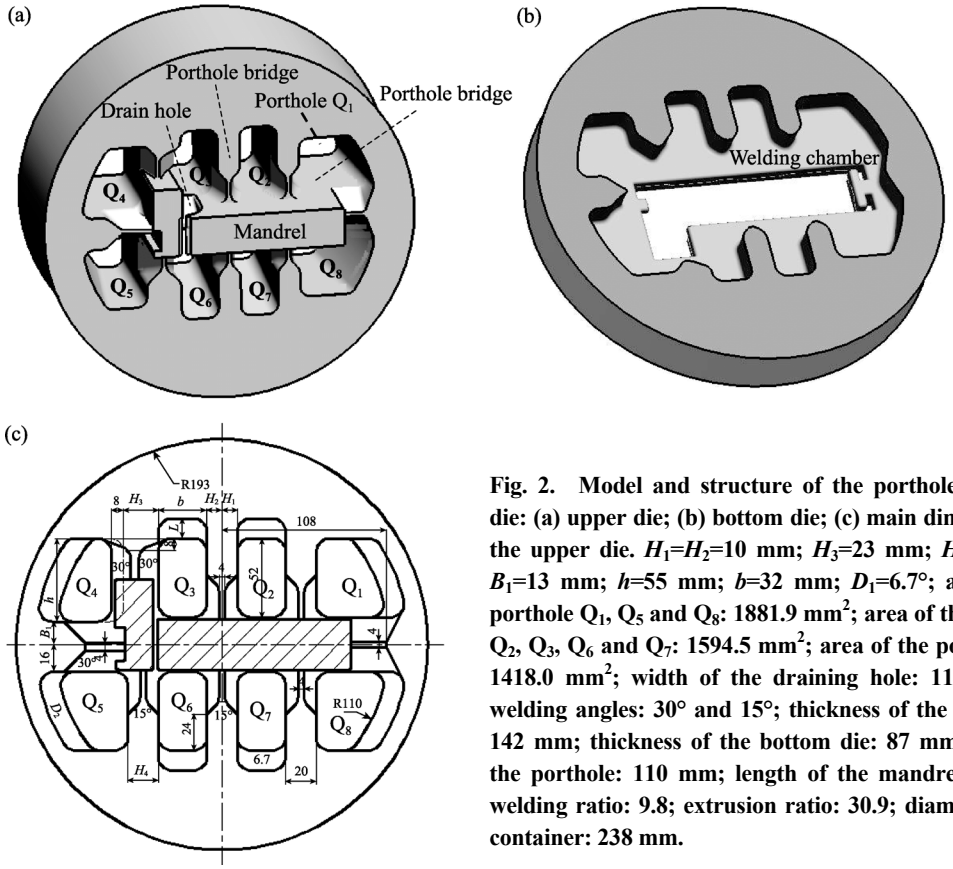

Fig. 2. Model and structure of the porthole extrusion die: (a) upper die; (b) bottom die; (c) main dimensions of the upper die. H_1=H_2=10 mm; H_3=23 mm; H_4=20 mm; B_1=13 mm; h=55 mm; b=32 mm; D_1=6.7°; area of the porthole Q_1, Q_5 and Q_8: 1881.9 mm^2; area of the porthole Q_2, Q_3, Q_6 and Q_7: 1594.5 mm^2; area of the porthole Q_4: 1418.0 mm^2; width of the draining hole: 11 mm. The welding angles: 30° and 15°; thickness of the upper die: 142 mm; thickness of the bottom die: 87 mm; depth of the porthole: 110 mm; length of the mandrel: 32 mm; welding ratio: 9.8; extrusion ratio: 30.9; diameter of the container: 238 mm.

The friction of the Al alloy and the die is assumed as a shear friction model, and the friction factor is defined as $m = \sqrt{3}\frac{\tau}{\sigma}$ (where τ is the shear stress of contact friction and σ the flowing stress) [15]. The m is set as 1 according to the ring compression test of the alloy at high temperature.

Under the industrial production conditions, the initial temperatures of the billet, container, die, and pressure pad are set as 500, 420, 480, and 30°C, respectively. The punch velocity is 2 mm/s.

2.2. Reconstruction of finite element meshes

The FEM geometry model of the die (as shown in Fig. 2) was built using the Pro/Engineer software and imported into the Deform-3D to numerically simulate. According to the reconstruction technology proposed by the authors [13-14], the reconstruction or repair method of the penetrated meshes of 9 welding planes in the welding stage is introduced as follows.

(1) When the volumes of the mesh penetration region and the unfilled region are almost equal, the meshes near the welding plane are transformed into a 3D geometry model composed of small triangle facets, *i.e*., the stereolithography (STL) model.

(2) By adopting the facet feature function of Pro/Engineer, the penetrated or aberrant triangle facets of the STL model are deleted, and the adjacent three points are selected to reconstruct triangle facets for filling the surfaces.

(3) The unfilled regions near the welding planes are also filled with a triangle facet, thus the penetrated region and the unfilled region form a 3D geometry model composed of small triangle facets.

(4) Importing the reconstructed geometry model into Deform-3D and adding elements and nodes, the simulation was continued.

The mesh model before and after being reconstructed is shown in Fig. 3.

In consideration of the calculation speed and accuracy, different sizes of meshes in different regions are set during the simulation, as shown in Fig. 4. The mesh sizes of the metal in the container, near the entrance of the portholes, near the porthole bridge, in the welding chamber, and near the orifice are set as 30, 3, 7, 3, and 1 mm, respectively.

3. Simulation results and analysis

3.1. Flowing behaviors of the metal

Fig. 5 exhibits the metal flowing behaviors at various

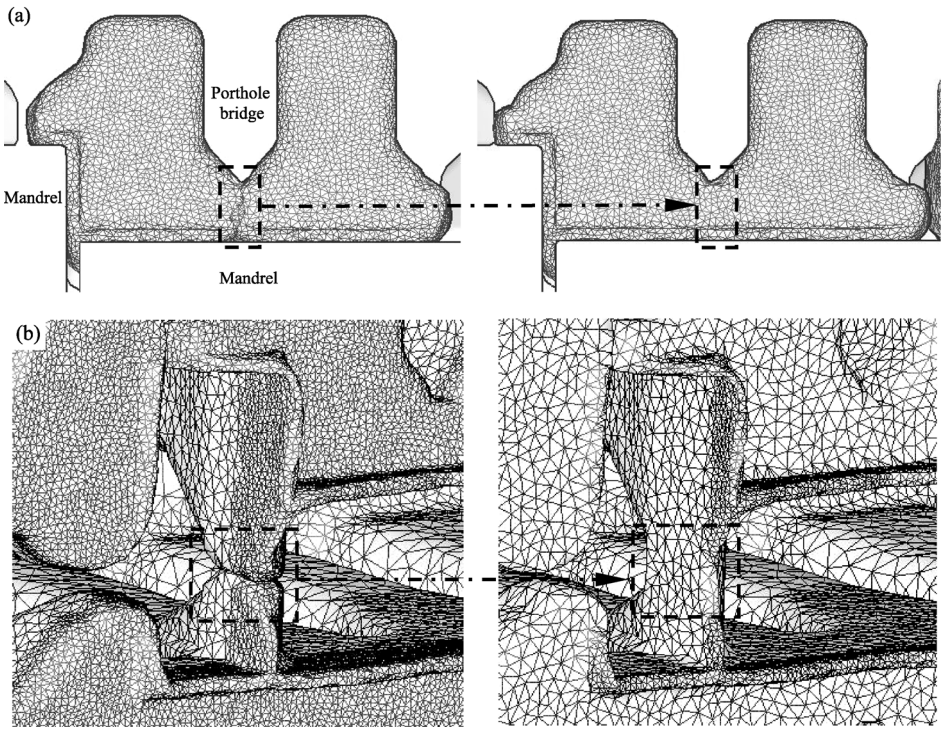

Fig. 3. Mesh reconstruction of welding-planes: (a) underneath the porthole bridge; (b) inside the drain hole.

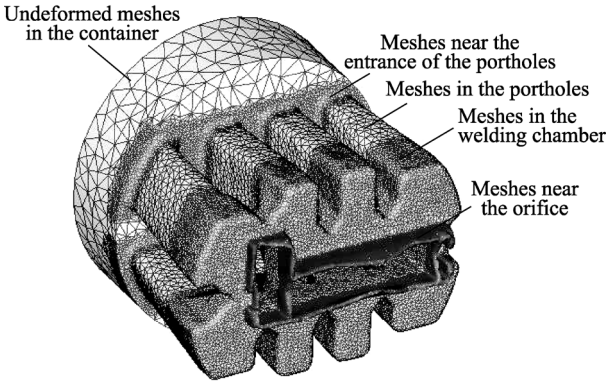

Fig. 4 Different sizes of the meshes in various regions.

extrusion strokes (*S*). Fig. 5(a) shows the condition as the metal flows into the portholes (diversion stage). Figs. 5(b)-(e) show the conditions as the metal fills the chamber and begins welding (welding stage). Fig. 5(f) shows the condition as the metal flows out of the die orifice and forms a hollow section (shape-forming stage).

At the diversion stage (Fig. 5(a)), the metal is divided into eight streams by porthole bridges and then flows into the portholes. The velocities of the metals in the central portholes (Q_2, Q_3, Q_6 and Q_7) are higher than those in the outside portholes (the values of the velocities are shown in Fig. 6) because of the lower friction resistance of the central

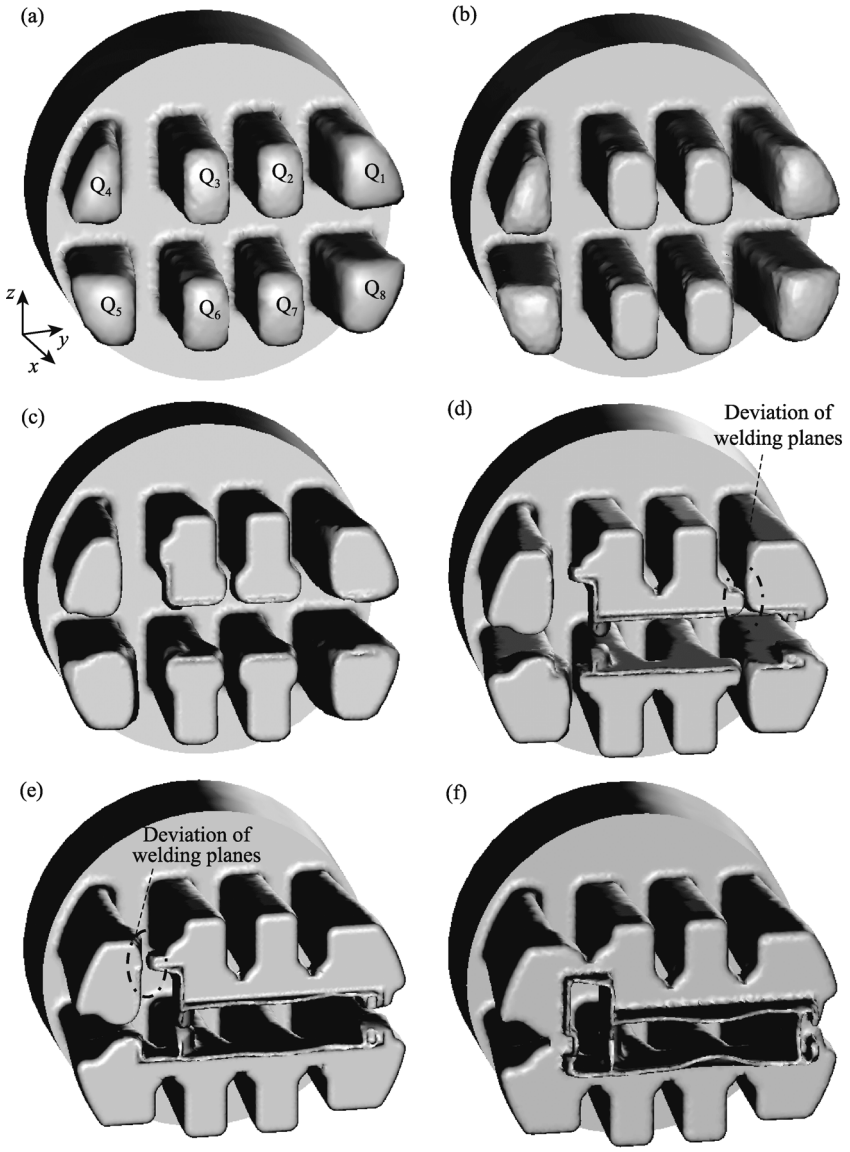

Fig. 5. Metal flowing behaviors in various extrusion stages: (a) flowing into the portholes (*S*=29.6 mm); (b) filling the welding chamber (*S*=39.1 mm); (c) filling the welding chamber (*S*=47.9 mm); (d) welding of the metal below the porthole bridge (*S*=50.3 mm); (e) welding of the metal in the drain hole (*S*=50.9 mm); (f) flowing out of the die orifice (*S*=52.0 mm).

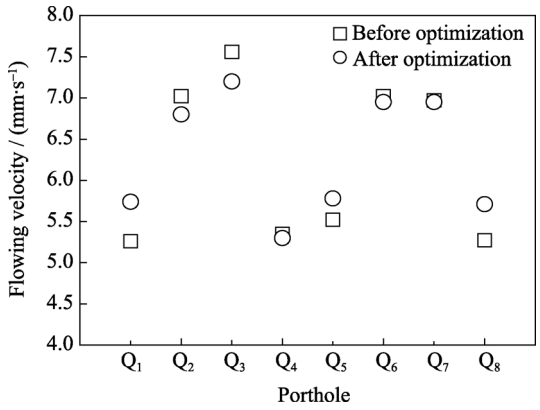

Fig. 6. Flowing velocities of the metal in portholes.

metal caused by the container than that of the outside metal. So, the central streams are longer than the outside streams.

At the welding stage, the eight streams of the metal contact with the bottom of the welding chamber successively. Surrounding the mandrels, the streams flow radially and fill the welding chamber. Because of the longer length, the four central streams contact with the bottom of the chamber firstly (Figs. 5(b) and (c)) and accomplish the welding stage firstly (Fig. 5(d)).

Moreover, Fig. 5(d) indicates that the welding planes of Q_2/Q_1 and Q_7/Q_8 deviate from the symmetry planes of the porthole bridge. The main reason is that the velocities of the central streams are higher than those of the outside streams, *i.e.*, the velocities of the metal in Q_2 and Q_7 are higher than those in Q_1 and Q_8. Fig. 5(e) indicates that when the streams flowing from the drain hole begin welding, the streams flowing from Q_1 and Q_8, Q_3 and Q_4, and Q_4 and Q_5 still do not contact each other. Meanwhile, because a part of the metal is extruded out of the die orifice, the velocities of the central streams are higher, which leads to the welding planes deviating from the symmetry plane of the welding planes of Q_3 and Q_4.

At the stage of shape-forming (Fig. 5(f)), the asymmetry flowing of the metal in the welding stage continues. In the various regions of the cross section, the velocities and lengths of the extruded metal are different, leading to the wavelike defect near the central region of the cross section.

3.2. Influence of the porthole configuration on the flowing velocity of the metal in the stage of filling the welding chamber

During the divergent extrusion of the hollow section, the configuration of the portholes (including the area and the position of every porthole) is one of the main factors to balance the metal flowing velocities and volumes and to determine whether the metals begin welding simultaneously as well as whether the flowing velocities of the cross section are uniform.

To eliminate the defects such as warp, twist, or wavelike caused by the discordant flowing velocities of the metal, it is necessary to ensure that the metals at two sides of the welding plane weld simultaneously as possible. For the conditions shown in Fig. 5, it means to decrease the velocities of the four central streams and increase the velocities of the four outside streams. For this purpose, the following optimization scheme is adopted on the basis of the FEM simulation results. The width of both Q_2 and Q_7 (b marked in Fig. 2(c)) is decreased from 32 to 30 mm, *i.e.*, the area of both Q_2 and Q_7 is 1505.1 mm^2; H_1 and h (refer to Fig. 2(c)) are increased from 10 to 13 mm and from 55 to 58 mm, respectively; The expanding angle D_1 of the outside four portholes is decreased from 6.7° to 5.2°; H_2, H_3, and B_1 are decreased to 7, 20, and 10 mm, respectively; and H_4 is increased to 25 mm.

In the diversion stage, the streams velocities in various portholes before and after optimization are exhibited in Fig. 6. It indicates that the velocities of the four outside streams (in portholes Q_1, Q_4, Q_5, and Q_8) increase obviously after optimization, which decreases the difference between the velocities of central and outside streams. So the streams contact the welding chamber bottom simultaneously, and the flowing uniformity of the metal in the stage of filling welding chamber was improved.

3.3. Influence of the porthole configuration on the position of welding planes

Fig. 7 shows the positions of the metal planes before and after the optimization of the porthole configuration. Fig. 7(a) indicates that, as the metal streams flowing from Q_2/Q_3 and Q_6/Q_7 begin welding (in the regions of z and f), the streams flowing from other portholes (in the regions of s, c, d, e, f, a, b, and g) do not contact. After the optimization as mentioned in Section 2.2, when the streams in the regions of z and f begin welding, the metal streams in the regions of g, d, and e contact, and the distances between two streams in the regions of c, b, and s are shortened obviously, as shown in Fig. 7(b).

The velocities of metal streams at the two sides of the welding plane are listed in Table 1. It demonstrates further that the flowing uniformity of the metal is improved obviously after the configuration optimization.

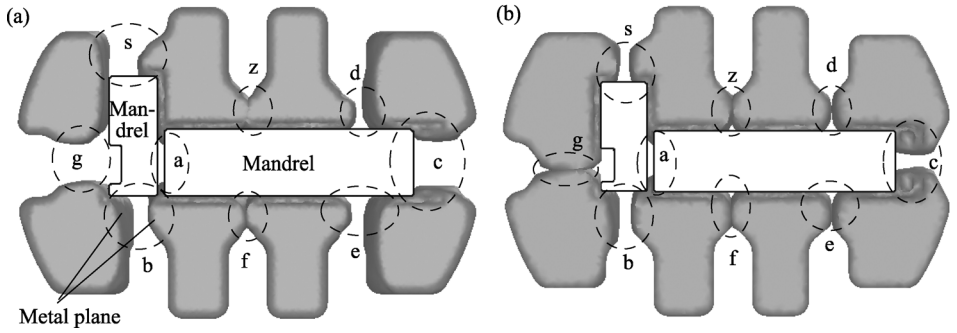

Fig.7. Positions of the metal planes: (a) before optimization; (b) after optimization.

Comprehensively, the flowing velocities and volumes of the metal streams are matching reasonably after the optimization. The deviation of welding planes from the symmetry planes of the porthole bridge is avoided, which is beneficial for improving the uniformity of the metal flowing velocities and eliminating the warp or wavelike defects. The shapes of the extruded section before and after the optimization are shown in Fig. 8.

3.4. Temperature distribution of the cross section

Compared with the traditional numerical simulation technology, the method proposed in this paper is more feasible to simulate the temperature distribution during the divergent extrusion of the hollow section, including the welding stage.

The temperature distributions of the cross section near the die orifice before and after optimizing the size of die construction are shown in Fig. 9. Before the optimization, the temperature of region I of the cross section (507-512°C) is lower than that of other regions (512-522°C). After the optimization, the temperature of region Ⅱ of the cross section (508-515°C) is lower than that of other regions (515-522°C). Because of the increase in the area of Q_4 after optimization, the friction surface increases, which makes the temperature of region I increase. Meanwhile, because the drain angles of Q_1 and Q_8 are decreased, the friction surface decreases, which makes the temperature of region Ⅱ decrease.

Table 1. Flowing velocities of the metal streams at two sides of the welding planes **mm·s^{-1}**

Position	Before optimization	After optimization
a, T	5.95	5.72
a, B	5.75	5.70
s, L	3.46	6.21
s, R	6.14	5.68
z, L	6.41	6.37
z, R	7.79	6.68
d, L	7.72	6.27
d, R	4.82	7.62
g, T	2.41	5.46
g, B	2.97	5.38
c, T	3.70	5.93
c, B	3.72	5.89
b, L	5.24	5.72
b, R	6.08	5.38
f, L	5.34	6.54
f, R	6.13	6.71
e, L	6.52	6.35
e, R	4.72	7.71

Note: L, R—metal planes at the left and right sides of the welding plane, respectively; T, B—metal planes at the upper and bottom sides of the welding plane, respectively.

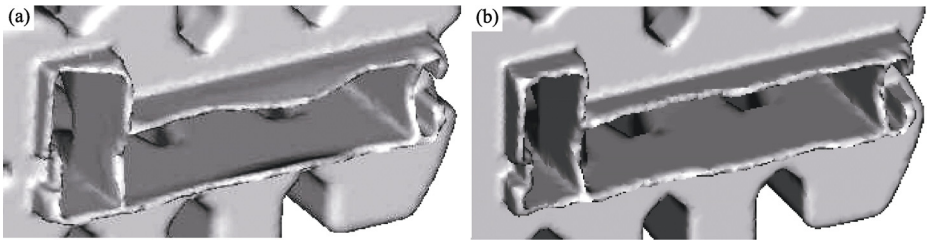

Fig. 8. Shapes of the extruded section in the shape forming stage: (a) before optimization; (b) after optimization.

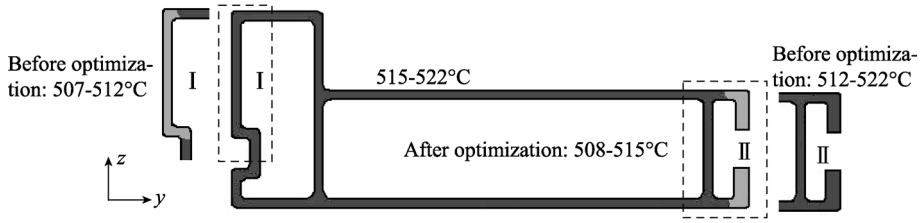

Fig. 9. Temperature distribution of the cross section near the die orifice.

The metal in region Ⅱ(C-type notch) is easier to be extruded from the die orifice because the thickness of the region is larger than that of other regions of the cross section. After the optimization, the temperature of region Ⅱ is 7-14°C lower than that of other regions, which means the deformation resistance of the region is higher. It counteracts the effect of the "easier to be extruded" mentioned above, which is beneficial for improving the uniformity of the flowing velocities of the metal on the cross section.

4. Conclusions

(1) By adopting the Deform-3D software and applying the reconstruction technology of welding-plane meshes proposed by the authors of the paper, the whole extrusion process (including the welding stage) of the hollow section with a complicated cross section was simulated.

(2) Based on the analyses of the metal flowing behaviors, the local die construction of the complicated cross section was optimized, including adjusting the porthole area, expanding the angle and the distance between the porthole and the container axis, *etc*. After the optimization, the flowing velocities and volumes of the metal streams match reasonably, and the warp or wavelike defect is avoided.

(3) The temperature distribution of the cross section was predicted. After the optimization, the surface temperature of the section distributes uniformly, and the temperature of the region with a larger thickness is 7-14°C lower than that of other regions, which is beneficial for improving the uniformity of the flowing velocities of the metal on the cross section.

References

[1] J.X. Xie and J.A. Liu, *Theory and Technology of Metal Extrusion*, Metallurgical Industry Press, Beijing, 2001, p.33.

[2] S. Murakami, Adoption of aluminum extrusion and its technology, *J. Jpn. Soc. Technol. Plast*., 567(2008), No.49, p.25.

[3] L.Q. Di and S.H. Zhang, Porthole die extrusion process numerical simulation and optimal die design, *J. Plast. Eng*., 16(2009), No.2, p.123.

[4] H.H. Jo, S.K. Lee, C.S. Jung, and B.M. Kim, A non-steady state FE analysis of Al tubes hot extrusion by a porthole die, *J. Mater. Process. Technol*., 173(2006), No.2, p.223.

[5] H.H. Jo, S.K. Lee, S.B. Lee, and B.M. Kim, Prediction of welding pressure in the non-steady state porthole die extrusion of Al7003 tubes, *Int. J. Mach. Tools Manuf*., 42(2002), No.6, p.753.

[6] M.L. Jung, M.K. Byung, and G.K. Chung, Effects of chamber shapes of porthole die on elastic deformation and extrusion process in condenser tube extrusion, *Mater. Des.*, 26(2005), No.4, p.327.

[7] G. Liu, J. Zhou, and J. Duszczyk, FEM analysis of metal flow and weld seam formation in a porthole die during the extrusion of a magnesium alloy into a square tube and the effect of ram speed on weld strength, *J. Mater. Process. Technol*., 200(2008), No.1-3, p.185.

[8] D.Y. Yang, K. Park, and Y.S. Kang, Integrated finite element simulation for the hot extrusion of complicated Al alloy profile, *J. Mater. Process. Technol*., 111(2001), No.1-3, p.25.

[9] L. Donati and L. Tomesani, The prediction of seam welds quality in aluminum extrusion, *J. Mater. Process. Technol.*, 153(2004), No.10, p.366.

[10] D.Y. Yang and K.J. Kim, Design of processes and products through simulation of three-dimensional extrusion, *J. Mater. Process. Technol*., 191(2007), No.1-3, p.2.

[11] L. Li, H. Zhang, J. Zhou, *et al*., Numerical and experimental study on the extrusion through a porthole die to produce a hollow magnesium profile with longitudinal weld seams, *Mater. Des*., 29(2008), No. 6, p.1190.

[12] X.H. Wu, G.Q. Zhao, Y.G. Luan, and X.W. Ma, Numerical simulation and die structure optimization of an aluminum rectangular hollow pipe extrusion process, *Mater. Sci. Eng. A*, 435(2006), No.5, p.266.

[13] J.X. Xie, D.N. Huang, J.Y. Li, and Z.H. Zhang, *A Method for Simulating Welding Process of Hollow Profile Extrusion with Porthole Die*, Chinese Patent, CN101604350A, 2009-12-16.

[14] D.N. Huang, J.Y. Li, Z.H. Zhang, and J.X. Xie, The metal flowing behaviors during the diplopore extrusion of square tube by a porthole die, *Trans. Nonferrous Met. Soc. China*, 20(2010), No.3, p.488.

[15] T. Chanda, J. Zhou, L. Kowalski, and J. Duszczyk, 3D FEM simulation of the thermal events during AA6061 aluminum extrusion, *Scripta Mater*., 41(1999), No.2, p.195.